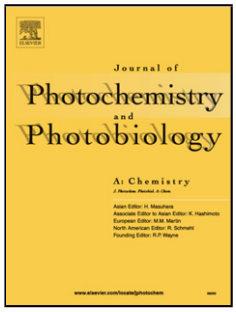

Title: Selective and Sensitive Off-On Probes specific for Palladium detection and Their Application in Biological Environments

Author: Ying Long Yin-juan Bai Jia Zhou Bing-qin Yang

PII: S1010-6030(16)30525-1
DOI: http://dx.doi.org/doi:10.1016/j.jphotochem.2016.09.022
Reference: JPC 10374

To appear in: *Journal of Photochemistry and Photobiology A: Chemistry*

Received date: 29-6-2016
Revised date: 19-9-2016
Accepted date: 21-9-2016

Please cite this article as: Ying Long, Yin-juan Bai, Jia Zhou, Bing-qin Yang, Selective and Sensitive Off-On Probes specific for Palladium detection and Their Application in Biological Environments, Journal of Photochemistry and Photobiology A: Chemistry http://dx.doi.org/10.1016/j.jphotochem.2016.09.022

Selective and Sensitive Off-On Probes specific for Palladium detection and Their Application in Biological Environments

Ying Long, Yin-juan Bai, Jia Zhou, Bing-qin Yang*

Key Laboratory of Synthetic and Natural Functional Molecule Chemistry, Ministry of Education, College of Chemistry and Materials Science, Northwest University, Xi'an 710127, PR China

Highlights:

- Two rhodamine-based Pd^{2+} fluorescence probes have been designed, synthesized and characterized.
- The probes exhibited highly selective Pd (II) - enhanced absorbance and fluorescence emission above 540 nm in ethanol-water (4/6, v/v, 20mmol/L HEPES, pH 7.4) by a reversible way.
- They can respond to Pd^{2+} directly (without supported reagents) and rapidly (completed within 1min).
- The two probes were conducted to cytotoxicity and bioimaging studies by HepG2 living cells and living mice indicated that they were low cytotoxic, cell permeable and can be used to detect Pd^{2+} in living systems.

Abstract: Two rhodamine B derivatives **ROP** and **ROM** have been rationally designed, synthesized and characterized. The probes exhibited highly selective Pd (II) - enhanced absorbance and fluorescence emission above 540 nm in ethanol-water (4/6, v/v, 20mmol/L HEPES, pH 7.4) by a reversible way. Upon the addition of Pd (II), the rhodamine spirolactam ring was unfolded and a 1:1 metal-ligand was formed, which can be used for "naked-eyes" detection. In addition, cytotoxicity and bioimaging studies by HepG2 living cells and living mice indicated that the probes were negligible cytotoxicity, cell permeable and suitable for detecting Pd (II) in biological environments.

Keywords: Rhodamine B; Palladium fluorescence probe; Cytotoxicity; Bioimaging

1. Introduction

Palladium belongs to the platinum-group elements (PGEs; consist of Pt, Pd, Ru, Rh, Ir and Os). It is widely used in various materials such as catalysts, dental crowns, jewelry and fuel cells [1-3]. Pd-catalyzed reactions such as Heck, Sonogashira, Buchwald–Hartwig and Suzuki–Miyaura reactions represent powerful transformations for the synthesis of complex molecules, which played an significant role in pharmaceuticals [4 -11]. However, their fruitful and frequent use can also generate a high level of residual palladium, which may result in the contamination of soil and water systems [11]. And, palladium can cause severe skin and eye irritation [12] when it is taken into human bodies via contaminated food, medicine, and water [13]. DNA, proteins, and other biomacromolecules, such as vitamin B6, have been reported to be able to strongly bind palladium ions, which may lead to a variety of cellular dysfunction processes [14] and therefore could cause health hazard [15-17]. Therefore, palladium detection both in the living and the environment has attracted tremendous attention. Detecting the content of palladium in samples was usually carried out by atomic absorption/emission spectroscopy (AAS/AES), ion-coupled plasma emission-mass spectroscopy (ICP-MS), solid-phase microextraction high performance liquid chromatography (SPME-HPLC), and X-ray fluorescence spectroscopy (XRF) [18-19]. Although these conventional methods provide an extremely and rapidly sensitive analysis, they need sophisticated sample-pretreatment procedures, complicated instrumentation and rigorous experimental conditions, which may restrict their extensive applications.

Fluorescent probe has become a widely used and important tool for monitoring metal ion concentration in biological samples. Most reported fluorescence probes have a metal chelating site linked to a fluorophore, and the metal binding causes the change in fluorescence intensity [20-25]. The development of synthetic receptors which are capable of recognising important metal ions (especially transition-metal ions) biologically and environmentally have attracted widespread interests from biologists, chemists,

environmentalists and clinical biochemists in recent years [26–31]. Fluorescent and colorimetric chemosensors have been increasingly applied in palladium analysis [32-34]. However, plenty of palladium detection fluorescence probes are defective: 1) through fluorescence quenching way [35-41]; 2) via irreversible reactions and even need supported reagents [42-44]; 3) colorimetric chemosensor and no fluorescence [45]; 4) the recognition reaction conditions are relatively strict and have a long response time [46-47]; 5) unsuitable for bioimaging applications [42-43,48]. Therefore, nowadays, design and synthesis palladium fluorescence probes which are capable of overcoming the above shortcomings are still have realistic significance.

Rhodamines are dyes widely employed in the study of complicated biological systems as fluorescence probes due to their high fluorescence quantum yields, high absorption coefficients, long-wavelength emissions and absorptions [49]. Owing to the rhodamines with a spirolactam scaffold, which undergoes the conformational transformation from the spirolactam (nonfluorescent and colorless) to an open-ring structure (fluorescent and colored), they have been widely applied in the design of vast chemical sensors in recent years, and these new designed chemosensors have been quoted in recently excellent review articles [50-53]. In spirocyclic form, the sensing event occurs in its five-membered lactam moiety. Obviously, these properties still present abundant opportunities to design new fluorescent probes. Herein, our research work contains the design, synthesis, structure characterizations, spectra characterizations and biological applications of fluorescent chemosensors for selective sensing of Pd^{2+}. In our previous work [54], we reported a fluorescent probe **T1**, which are successfully applied in Pd^{2+} detection. Based on the successful experimental results, we try to follow and expand this research, so, here two novel rhodamine-based chemosensors **ROP** and **ROM** were prepared by three-step synthesis using inexpensive materials. Especially, these chemosensors showed highly selective and sensitive fluorescence "turn-on" and enhanced behaviors toward Pd^{2+} followed the remarkable color changes from colorless to pink, which can be used for "naked-eyes" detection. And, these probes can give highly selective spectroscopic responses to Pd^{2+} over other metal ions in ethanol-water (4/6, v/v, 20mmol/L HEPES, pH 7.4) media by reversible way. Importantly, **ROP** and **ROM** can respond to Pd^{2+} directly (without supported reagents) and rapidly (completed within 1min) with high sensitivity (DL=3.49 μmol/L, 4.64 μmol/L, respective). Moreover, the two probes were conducted to cytotoxicity and bioimaging studies by HepG2 living cells and living mice indicated that the probes were low cytotoxic, cell permeable and can be used to detect Pd^{2+} in living systems.

2. Experimental

2.1 materials

All the solvents and reagents were of analytic grade and they were used without further purification unless for special needs. The **ROP** and **ROM** were dissolved in DMF-EtOH (1/40, v/v) solution in concentration of 1mmol/L as stock solutions. And then took out quantificational **ROP** and **ROM** in different testing system. We used the HITACHI F-4500 fluorescence spectrophotometer to measure the fluorescence spectra. And the absorbance spectra measurements were also performed on a Shimadzu UV-1700 spectrophotometer. IR spectra were on a Bruker Tensor 27 spectrometer. NMR spectra were recorded on a Varian INOVA-400 MHz spectrometer (at 100 MHz for ^{13}C NMR and 400 MHz for ^{1}H NMR). A Bruker micro TOF-Q II ESI-TOF LC/MS/MS Spectroscopy was used to perform mass spectra. Melting points were taken on an XT-4 micromelting apparatus and uncorrected. Results of cytotoxicity were analyzed with the Soft max pro software (version 2.2.1) in Spectra max190-Molecular Devices. And the living cells imaging were performed on an Olympus FV1000 conf-ocal microscopy, we set the excitation wavelength as 540 nm. The living animals imaging were conducted on IVIS DPECTRUM, with an excitation filter 550 nm and an emission range = 580-600 nm. All reagent used for synthesis were of analytical-reagent grade and commercially available from Aldrich. Thin-layer chromatography (TLC) and column flash chromatography was performed on silica gel GF254 and Merck silica gel (250–400 mesh ASTM), respective. And the twice-distilled water was used throughout the experiment.

2.2 Synthetic procedures

*2.2.1 Synthesis of Compound **2***

We synthesized the compound **2** from Rhodamine B by the procedures published in literatures [55-58].

*2.2.2 Synthesis of Compound **3***

As literature [59] reported that Compound **3** was synthesized by condensing Rhodamine hydrazide with o-phthalaldehyde. However, we have optimized the experimental conditions in order to reduce by-products and improve the conversion rate, so, instead of refluxing Rhodamine hydrazide with o-phthalaldehyde in ethanol, we let the condensation reaction of Rhodamine hydrazide and o-phthalaldehyde occur at room temperature. To a 250 mL round bottom flask, an excess of o-phthalaldehyde (0.804 g, 0.006 mol) was dissolved in 20 mL ethanol, cooled with a cold water bath. Then Rhodamine hydrazide (1.369g, 0.003 mol) was dissolved in 150 mL ethanol and added dropwise to the above 250 mL flask within 30 min with vigorous stirring, and the stirred mixture was allowed to stand in the cold water bath for about 4 h, then the solvent was removed under reduced pressure, further purified the resulting precipitate by silica gel column chromatography to give **3** (light yellow solid) in 91.6% yield. MS Calcd for ($C_{36}H_{36}N_4O_3$) m/z = 572.2787, Found: 573.2864 $(M+H)^+$. IR (KBr) υ: 1750, 1690, 1635, 1517, 1306, 1271, 1239, 1213, 1118, 818, 786, 756, 699 cm^{-1}. ^1H NMR (400 MHz, $CDCl_3$, TMS), δ (ppm): 1.13 (12H, t, J = 8 Hz), 3.27~3.33 (8H, m), 6.32~6.41 (2H, m), 6.57~6.62 (4H, m), 7.04 (1H, d, J = 8 Hz), 7.32 (1H, t, J = 8 Hz), 7.49~7.53 (3H, m), 7.68 (1H, d, J = 8 Hz), 7.96 (1H, d, J = 8 Hz), 8.12 (1H, d, J = 8 Hz), 9.13 (1H, s), 9.78 (1H, s).Anal. calcd. for $C_{36}H_{36}N_4O_3$ (%): C, 75.5; H, 6.34; N, 9.78. Found: C, 75.7; H, 6.39; N, 9.81.

*2.2.3 Synthesis of Compound **ROP** and **ROM***

Synthesis of Compound ROP: Compound **3** (0.572 g, 0.001mol) was dissolved in 20ml ethanol. Then a solution of 2-aminophenol (0.131g, 0.0012mol, a little excess) in ethanol (20 mL) was added and the mixture was stirred for 8 h at ambient temperature. Then filtered the precipitate produced and washed 3 times with 10 mL cold ethanol. After drying under reduced pressure, the crude product was purified by recrystallization in $EtOH/H_2O$ to give Compound **ROP** (light yellow solid) in 83.4% yield. mp: 188~190 °C. MS Calcd for ($C_{42}H_{41}N_5O_3$) m/z = 663.3209, Found: 664.3294 $(M+H)^+$. IR (KBr) υ: 3388, 2969, 1698, 1616,1546, 1513, 1423, 1326, 1268, 1222, 1120, 1074, 1018, 979, 869, 819, 786, 757, 719, 646, 534, 472 cm^{-1}.^1H NMR (400 MHz, $CDCl_3$, TMS), δ (ppm): 1.13 (12H, t, J = 8 Hz), 3.31~3.37 (8H, m), 6.22~6.24 (2H, m), 6.44~6.47 (4H, m), 7.03~7.05 (1H, m), 7.34~7.37 (1H, m), 7.39~7.486 (4H, m), 7.56~7.61 (1H, m), 7.83~8.16 (4H, m), 8.04 (1H, s), 10.75 (1H, s). ^{13}C NMR (100 MHz, $CDCl_3$, TMS), δ (ppm): 12.6, 44.3, 55.1, 66.0, 97.9, 98.9, 103.9, 104.9, 107.9, 123.2, 127.7, 133.9, 143.4, 149.0, 152.1, 166.5. Anal. calcd for $C_{42}H_{41}N_5O_3$ (%): C, 75.99; H, 6.23; N, 10.55. Found: C, 76.02; H, 6.22; N, 10.57.

Synthesis of Compound ROM: Compound **3** (0.572 g, 0.001mol) was dissolved in 20mL methanol. Then a solution of o-aminoanisole (0.148g, 0.0012mol, a little excess) in ethanol (20 mL) was added and the mixture was stirred for 8 h at room temperature. Then filtered the precipitate produced and washed 3 times with 10 mL cold ethanol. After drying under reduced pressure, The crude product was purified by recrystallization in $EtOH/H_2O$ to give Compound **ROM (**pale yellow powder) in 80.6% yield. mp: 113~115 °C. IR (KBr) υ: 3437, 2972, 2927, 2873, 1727, 1697, 1613, 1518, 1464, 1419, 1301, 1266, 1222, 1118, 1078, 1020, 975, 818, 783, 759, 695, 530 cm^{-1}. MS calcd for ($C_{43}H_{43}N_5O_3$) m/z = 677.3366, Found: 678.3428 $(M+H)^+$. ^1H NMR (400 MHz, $CDCl_3$), δ (ppm): 1.17 (12H, t, J = 8 Hz), 3.33~3.39 (8H, m), 3.75 (3H, s), 6.23~6.26 (2H, m), 6.43~6.49 (4H, m), 7.04 (1H, d, J = 4 Hz), 7.37~7.39 (1H, m), 7.42~7.49 (4H, m), 7.59 (1H, d, J = 4 Hz), 7.86 (1H, d, J = 4 Hz), 7.95 (1H, d, J = 4 Hz), 8.05 (1H, d, J = 4 Hz), 8.17 (1H, d, J = 8 Hz), 9.56 (1H, s), 10.78 (1H, s). ^{13}C NMR (100MHz, $CDCl_3$), δ (ppm): 12.6, 44.3, 55.9, 66.4, 97.9, 105.9, 115.1, 115.9, 120.1, 122.7, 129.0, 133.5, 135.3, 135.9, 136.2, 145.9, 148.9, 151.5, 156.6, 165.0. Anal. calcd for $C_{43}H_{43}N_5O_3$ (%): C, 76.19; H, 6.39; N, 10.33. Found: C, 76.20; H, 6.38; N, 10.35.

2.3 Preparation of the test solution

The 10 μmol/L test solution of probes **ROP** and **ROM** were prepared in ethanol-water (4/6, v/v, 20mmol/L HEPES, pH 7.4). The solutions of various testing cation species were prepared from $CaCl_2$, $AgNO_3$, $MgCl_2$, $CoCl_2·6H_2O$, $CdCl_2$, $ZnCl_2$, $CuCl_2·2H_2O$,

$MnSO_4·H_2O$, $HgCl_2$, $NiCl_2·6H_2O$, $Pb(NO_3)_2$, $CrCl_3·6H_2O$, $PdCl_2$, $PtCl_2$, $BaCl_2·2H_2O$, NaCl, $AlCl_3·6H_2O$ and $FeCl_3·6H_2O$ dissolved in the double distilled water. Before spectroscopic measurements, the corresponding solutions of probes were freshly prepared by diluting the high concentration stock solutions. All the measurements were made according to the procedures as follows. Placing 1 mL of the probe solution and an appropriate aliquot of each metal stock into a 10 mL glass tube, and diluting the solution to 10 mL with ethanol-water (4/6, v/v, 20mmol/L HEPES, pH 7.4) solution. The absorbance was showed at 550 nm and the fluorescence emission appeared at 583 nm. Both the excitation and emission wavelength band passes were set as 5.0 nm and the excitation wavelength was set at 540 nm.

2.4 Cytotoxicity assay

The MTT (5-dimethylthiazol-2-yl-2, 5-diphenyltetrazolium bromide) assay was performed to evaluate the toxicity of **ROP**, **ROM** and Pd^{2+} by HepG2 cells [60]. 90% confluent cell were chosen, digested by 1 mL 0.25% of trypsin, and transferred in 96-well plates. The cells were treated and incubated at 37 °C under 5% CO_2 in culture medium (RPMI 1640 + 10% FBS) and maintained 24 h. Different concentrations of **ROP**, **ROM** and Pd^{2+} were added to the 96-well plates, respectively. Then another 24 h incubation was taken at the same condition. Following this, the medium was removed and washed three times with phosphate buffered saline (PBS). Then the medium was replaced with mixed liquor of MTT（5 mg/mL）and culture medium and incubated for an additional 4 h. After that, the MTT was removed and washed three times with PBS. Subsequently, 150 μL DMSO was carefully added to each well and ultrasonic oscillation for 10 minutes. All the experiments were conducted in triplicate. The cell viability (%) was calculated according to the Equation: Cell viability%= [OD490 (sample)/ OD490 (control)] ×100%, where OD490 (sample) represents the optical density of the wells treated with various concentration of probes or Pd^{2+} and OD490 (control) represents that of the wells treated with ethanol.

2.5 Cell culture and fluorescence imaging

The human cancer cell line HepG2 (liver cells) were cultured in RPMI 1640 replenished with 10% FBS. Before the experiments, cells were processed with probes **ROP** and **ROM** (10 μmol/L) for 1 h at 37 °C in humidified air and 5% CO_2, washed three times with PBS then imaged. After incubation with Pd^{2+} (10 μmol/L) for another 1.5 h at 37 °C, cells were washed 3 times with PBS to remove remaining Pd^{2+} and then imaged. Confocal fluorescence imaging was carried out with an Olympus FluoView FV1000 laser scanning microscope with 80× objective lens. Excitation of probe-loaded cells at 540 nm was performed with a solid laser and emission was collected at 550–750 nm.

2.6 Fluorescence imaging in living animals

Kun Ming mice (15-20g) were anesthetized by an injection of xylazine (10 mg/kg) and ketamine (80 mg/kg). Then, the mice were given an intraperitoneal (10 μmol/L, 5μL) injection of the probes **ROP** and **ROM**. After ten minutes, The mice were injected with Pd^{2+} (10 μmol/L, 5μL) and then imaged by using an IVIS imaging system with excitation and emission filters set at 550 nm and 580nm, respectively.

3. Results and discussion

3.1 Spectroscopic properties

The probes **ROP** and **ROM** exhibited prominent selective and sensitive response to Pd^{2+}. Hydroxy group and methoxy group moieties have effects on the fluorescence intensities. However, no obvious differences were found on the other spectral properties for the two probes. Thus, **ROP** was chosen for further discussion, optical spectra of **ROM** was shown in the Supporting Information.

It is an essential feature for a probe to have a high selectivity toward the analyte over the potentially competing species. Shift of fluorescence and absorbance spectra caused competition and selectivity by **ROP** in the presence of Pd^{2+} and other competitive metal ions were recorded in **Fig.1 a** and **b**, respectively. There was no obvious fluorescence changes were observed in the presence of other cations (**Fig.1c**), such as heavy and transition metal ions (Mn^{2+}, Pb^{2+}, Cd^{2+}, Co^{2+}, Fe^{3+}, Cu^{2+}, Ni^{2+}, Ag^{+}, Zn^{2+}, Cr^{3+}, Pt^{2+}, Hg^{2+}), alkali or alkaline-earth metals (Na^{+}, Ca^{2+},Mg^{2+}, Ba^{2+}) and Al^{3+}.

However, the F/F_0 value was more than 100-fold increase after the addition of Pd^{2+} at the same concentration. Moreover, Pd^{2+} caused remarkable enhancement in fluorescence and obvious color changes. The colorimetric and fluorometric behaviors of **ROP**+**Pd^{2+}** and **ROM**+**Pd^{2+}**complex could be conveniently distinguished from those of the free **ROP** and **ROM** by the naked eye, as shown in **Fig.2**. This strongly suggested **ROP** and **ROM** has high selectivity to divalent palladium ion and can serve as "naked- eyes" probes for Pd^{2+}.

Fluorescence and UV titration experiments were carried out for the sake of further investigating the interaction of **ROP** and Pd^{2+}. Since the stable "spirolactam form" of rhodamine, free **ROP** represents colorless and no fluorescence response in the range from 550 to 750 nm. However, upon gradual addition of Pd^{2+}, significant enhancement of fluorescence with an emission maximum at 583 nm (**Fig.3a**) and an absorbance maximum at 550 nm (**Fig.3b**) were observed. It was attributable to the delocalization effects in the xanthene moiety of the rhodamine. With the Pd^{2+} concentration increasing, a continuous increase of fluorescence intensity appeared. After adding more than 1.0 equiv of Pd^{2+}, the fluorescence intensity showed negligible changes (**Fig. 3a**, inset). The results clearly indicated that, owing to the addition of Pd^{2+} to **ROP**, the spirolactam form was unfolded, and formed a highly delocalized π-conjugated structure. Thus, obvious and significant enhancement of absorbance and fluorescence were observed.

The association constant K was calculated according to the Benesi–Hildebrand equation [61] : $(F_{max} - F_0)/(F_x - F_0) = 1 + (1/K)(1/[Pd^{2+}])$, where F_{max}, F_0 and F_x are fluorescence intensities of probe in the presence of Pd^{2+} at saturation, free probe, and any intermediate Pd^{2+} concentration (**Fig.4**). The binding constant value was found to be $K = 2.45 \times 10^4$ L/mol. The linearity of this plot ensures the formation of a 1:1 clathrate between **ROP** and Pd^{2+} (R=0.99338). When the fluorescence intensity reached the maximum of the probe **ROP** to Pd^{2+}, F/F_0 was as high as over 100-fold, demonstrating that **ROP** has the excellent capability of detecting Pd^{2+} both quantitatively and qualitatively.

It is well known that the spirolactam ring of the rhodamine derivative is open in acidic media and then exhibits the strong fluorescence of rhodamine. Therefore, it is necessary to evaluate the effect of pH on the fluorescence of **ROP**. The effects of pH were evaluated in the pH range from 2.0 to 12.0 (**Fig. 5a**). No obvious enhancement of fluorescence at 550 nm was observed within pH 5.0–12.0, suggesting that it was insusceptible to the change of acid–base solution. However, in the presence of Pd^{2+}, a remarkable fluorescence emission band at 583 nm was formed under different pH values. It showed the pH value corresponding to the highest response approximately in 5~10, which revealed that the probe **ROP** for Pd^{2+} could work well in approximate physiological conditions with a very low background response. Therefore, further studies were carried out in ethanol-water (4/6, v/v) at pH 7.4. Furthermore, the time-dependence of probe **ROP** fluorescence was also evaluated in the presence of Pd^{2+} ions. The results showed that, upon the reaction of probe **ROP** with Pd^{2+}, the fluorescence of all the tested solutions remarkably increased to their maximum value within the first 1 min. (**Fig.5b**).

3.2 Calculation of detection limit

The detection limit of **ROP** and **ROM** were determined from fluorescence titration data (**Fig.3a, Fig.S2a**) based on reported and broadly used method [62-64]: According to the results of titration experiments, graphs of **$(F_{min} - F) / (F_{min} - F_{max})$** versus **log $[Pd^{2+}]$** were plotted, where the **F** is the fluorescence intensity at 583 nm at each concentration of Pd^{2+} added, **F_{min}** and **F_{max}** are the minimum and maximum fluorescence intensity at 583 nm respectively. Linear regression curves were then fitted (**Fig.6**), and

the intercepts of the lines at x-axis were taken as detection limit of **ROP** (3.49 μmol/L) and **ROM** (4.64 μmol/L).

3.3 Reversibility and proposed mechanism for the binding of probes with Pd^{2+}

In this section, we only discuss the experimental results of **ROP** interacted with Pd^{2+}, the experimental results of **ROM** are depicted in Supporting Information.

As is well known, the reversibility is an important property to obtain an excellent probe. Thus, the EDTA–adding experiments were conducted to examine the reversibility of the probes **ROP**. As clearly shown in **Fig.7a**, the absorbance decreased when EDTA was added to the mixture containing **ROP** and Pd^{2+}. Besides, the color of mixture changed back to colorless and fluorescence intensity decreased. When Pd^{2+} was added to the system again, the signals were almost completely reproduced (**Fig. 7b**) and the colorless solution turned to pink. The above process can be repeated several cycles without significant changes in the fluorescence spectrum (**Fig.7b.insert**). These findings indicated that probe **ROP** is a reversible fluorescent probe toward Pd^{2+}.

Binding analysis using the method of continuous variations (Job's plot) was measured. A maximum absorbance at 550 nm (**Fig.8.insert**) and fluorescence emission at 583 nm (**Fig.8**) were observed when the molecular fraction of **ROP** are close to 0.5, which established the 1:1 complex formation between **ROP** and Pd^{2+}. Thus, the most likely binding sites for Pd^{2+} are the conjugated moieties including phenolic hydroxyl O, imino N, benzoyl hydrazine N and O atoms. And proposed binding modes between the probes **ROP&ROM** and Pd^{2+} are shown as **Scheme 2**. It is very likely due to the chelation–induced ring opening of rhodamine spirolactam, rather than other possible reactions [51, 65].

3.4 Cytotoxicity assays and biological imaging applications

To ascertain the cytotoxic effects of **ROP**, **ROM** and Pd^{2+}, the MTT assay was performed according to the reported method [60].The details of MTT experimental operations can be seen in Experimental section of this article. Data are expressed as mean ± standard deviation in **Table 1** (supporting information).The results were illustrated in **Fig.9**. The cell viability still remains 99.71%, 91.06%, 92.92% under the treatment of 25 μmol/L probes and Pd^{2+}, which indicated that **ROP**, **ROM** and Pd^{2+} are low cytotoxic to cells and suitable for bioimaging.

To further demonstrate the practical applicability of the probe in biological samples, fluorescence imaging experiments were conducted in living cells. The fluorescence images of HepG2 cells were recorded before and after addition of Pd^{2+}, shown in **Fig. 10**. In the absence of Pd^{2+}, free **ROP** and **ROM** showed no detectable fluorescence signal in living cells (**Fig. 10a**). By contrast, after incubation with Pd^{2+}, a bright fluorescence was observed in living cells (**Fig. 10c**). Bright-field transmission images of cells treated with Pd^{2+} and probe revealed that the cells were viable throughout the imaging experiments (**Fig. 10b**). The results suggested that probes **ROP** and **ROM** can penetrate the cell membrane and can be applied for in vitro imaging of Pd^{2+} in living cells and potentially in vivo.

Further research on the potential of biological imaging applications, fluorescence imaging in living mice was performed [66]. The probes **ROP** and **ROM** (10 μmol/L，5μL) was injected into the living mice and no fluorescence signal were noted (**Fig .11a**). After

ten minutes, as the Pd^{2+} injection, a large fluorescence signal was observed within a few minutes of injection (**Fig .11b**).This indicates the potential in vivo imaging applications of the probes.

4. Conclusion

In summary, we have described two novel rhodamine-based probes **ROP** and **ROM**, they can give selective and sensitive fluorescence enhancement response to Pd^{2+} via a reversible sensing mechanism in ethanol - water solution. High selectivity toward Pd^{2+} is exhibited and little cross-sensitivity is observed to other commonly metal ions. The molecular design might greatly contribute to the development of more efficient and useful probes based on rhodamine platform. The excellent biological values of probes are demonstrated by the cytotoxicity and fluorescence imaging in HepG2 living cells and living mice. It is anticipated that the probes will significantly promote the studies on the effects of Pd^{2+} in biological systems.

Acknowledgments

This work was supported by the National Natural Science Foundation of China (No. 21172178)

References

[1] J. Le Bars, U. Specht, J. S. Bradley, etal, A Catalytic Probe of the Surface of Colloidal Palladium Particles Using Heck Coupling Reactions *Langmuir* 1999, 15, 7621– 7625.

[2] T. Iwasawa, M. Tokunaga, Y. Obora, etal, Homogeneous Palladium Catalyst Suppressing Pd Black Formation in Air Oxidation of Alcohols *J. Am. Chem. Soc*. 2004, 126, 6554 –6555.

[3] M. Lafrance, K. Fagnou, Palladium-Catalyzed Benzene Arylation: Incorporation of Catalytic Pivalic Acid as a Proton Shuttle and a Key Element in Catalyst Design*J. Am. Chem. Soc*. 2006, 128, 16496 – 16497.

[4] G. Zeni, R. C. Larock, Synthesis of Heterocycles via Palladium π-Olefin and ð-Alkyne Chemistry *Chem. Rev*. 2004, 104, 2285 – 2309;

[5] C. Liu, S.K. Zhang, Y. X. Zhang, etal, Arylation of pyridine N-oxides via a ligand-free Suzuki reaction in water. *Chin. Chem. Lett*, 2015,01:55-57.

[6] L. F. Tietze, H. Ila, H. P. Bell, Enantioselective Palladium-Catalyzed Transformations *Chem. Rev*. 2004, 104, 3453 – 3516;

[7] K. C. Nicolaou, P. G. Bulger, D. Sarlah, Metathesis Reactions in Total Synthesis *Angew. Chem*. 2005, 117, 4516 – 4563; *Angew. Chem. Int. Ed*. 2005, 44, 4442 –4489.

[8]E.Rajanarendar, G.Mohan, E.Kalyan Rao,etal, Palladium-catalyzed Suzuki-Miyaura cross-coupling reaction of organoboronic acids with N-protected 4-iodophenyl alanine linked isoxazoles. *Chin. Chem. Lett*, 2009,01:1-4.

[9] X. Chen, K. M. Engle, D. H. Wang, etal, Palladium(II)-katalysierteC-H-Aktivierung/C-C-Kreuzkupplung: Vielseitigkeit und Anwendbarkeit *Angew. Chem.* 2009, 121, 5196 – 5217; Palladium(II)-Catalyzed C-H Activation/C-C Cross-Coupling Reactions: Versatility and Practicality *Angew. Chem. Int. Ed*. 2009, 48, 5094 –5115.

[10] M. Amini, M. Bagherzadeh,S. Rostamnia. Efficient imidazolium salts for palladium-catalyzed Mizoroki-Heck and Suzuki-Miyaura cross-coupling reactions[J]. *Chin. Chem. Lett*, 2013,05:433-436.

[11] V. F. Hodge, M. O. Stallard, Platinum and palladium in roadside dust *Environ. Sci. Technol.* 1986, 20, 1058 – 1060.

[12] Kielhorn J, Melber C, Keller D, et al. Palladium–a review of exposure and effects to human health [J]. International Journal of Hygiene and Environmental Health, 2002, 205(6): 417-432.

[13] Liu, B.; Wang, H.; Wang, T.; Bao, Y.; Du, F.; Tian, J.; Li, Q.; Bai, R.Chem. Commun.2012, 48, 2867−2869.

[14] (a) Gebel, T.; Lantzsch, H.; Plebow, K.; Dunkelberg, H.Mutat. Res., Genet. Toxicol. Environ. Mutagen.1997, 389, 183−190. (b) Wiseman, C. L. S.; Zereini, F.Sci. Total Environ.2009, 407, 2493−2500. (c) Spicer, C. D.; Triemer, T.; Davis, B. G.J. Am. Chem. Soc. 2012,134, 800−803.(d) Yusop, R. M.; Unciti-Broceta, A.; Johansson, E. M.V.; Sá nchez-Martín, R. M.; Bradley, M.Nat. Chem.2011, 3, 239−243.

[15] T. Z. Liu, S. D. Lee, R. S. Bhatnagar, Toxicity of palladium *Toxicol. Lett.* 1979, 4, 469 – 473.

[16] J. C. Wataha, C. T. Hanks, Biological effects of palladium and risk of using palladium in dental casting alloys *J. Oral Rehabil*. 1996, 23, 309 –320.

[17] International Programme on Chemical Safety. Palladium;Environmental Health Criteria Series 226, World Health Organization, Geneva, 2002.

[18] Meel KV, Smekens A, Behets M, etal, Determination of platinum, palladium, and rhodium in automotive catalysts using high-energy secondary target xray fluorescence spectrometry. *Anal Chem* 79:6383–6389.

[19] M. A. Taher, Z. Daliri, H. Fazelirad, Simultaneous extraction and preconcentration of copper, silver and palladium with modified alumina and their determination by electrothermal atomic absorption spectrometry. *Chin. Chem. Lett*, 2014,04:649-654.

[20] Park J, Rao B A, Son Y A. "Turn-on" fluorescent and colorimetric determination of Cu^{2+} ions in aqueous media based on a Rhodamine-N-phenyl Semicarbazide derivative [J]. Fibers and Polymers, 2015, 16(5): 953-960.

[21] X. H. Yang, S Li, Z. S. Tang, etal, A simple, water-soluble, Fe^{3+}selective fluorescent probe and its application in bioimaging. *Chin. Chem. Lett*, 2015,01:129-132.

[22] Liu J, Liu H, Pu S. A highly selective diarylethene-based fluorescent sensor for respective recognition of Zn^{2+} and F^{-} [J]. Journal of Photochemistry and Photobiology A: Chemistry, 2016, 324: 14-22.

[23] Qin J, Yang Z. Fluorescent chemosensor for detection of Zn^{2+} and Cu^{2+} and its application in molecular logic gate [J]. Journal of Photochemistry and Photobiology A: Chemistry, 2016, 324: 152-158.

[24] Z.X. Han, B.S. Zhu, T.L. Wu, etal, A fluorescent probe for Hg^{2+}sensing in solutions and living cells with a wide working pH range. *Chin. Chem. Lett*, 2014,01:73-76.

[25] Saini A K, Srivastava M, Sharma V, et al. A highly selective, sensitive and reversible fluorescence chemosensor for Zn^{2+} and its cell viability [J]. Dalton Transactions, 2016, 45(9): 3927-3935.

[26] T. Bura , R. Ziessel, Design, synthesis and redox properties of a fluorene platform linking two different Bodipy dyes *Tetrahedron Lett.* 2010, 51, 2875.

[27] Sun W, Guo S, Hu C, et al. Recent Development of Chemosensors Based on Cyanine Platforms [J]. Chemical reviews, 2016, 116(14): 7768-7817.

[28] Carter K P, Young A M, Palmer A E. Fluorescent sensors for measuring metal ions in living systems[J]. Chemical reviews, 2014, 114(8): 4564-4601.

[29] W. Y. Wong , P. D. Harvey, Recent Progress on the Photonic Properties of Conjugated Organometallic Polymers Built Upon the *trans*-Bis(*para*-ethynylbenzene)bis(phosphine)platinum(II) Chromophore and Related Derivatives *Macromol. Rapid Commun*., 2010, 31, 671.

[30] Jeong Y, Yoon J. Recent progress on fluorescent chemosensors for metal ions[J]. Inorganica Chimica Acta, 2012, 381: 2-14.

[31] Antina E V, Bumagina N A, V'yugin A I, et al. Fluorescent indicators of metal ions based on dipyrromethene platform[J]. Dyes and Pigments, 2017, 136: 368-381.

[32] Yang L, Wang C, Chang G, et al. Facile synthesis of new coumarin-based colorimetric and fluorescent chemosensors: Highly efficient and selective detection of Pd^{2+} in aqueous solutions [J]. Sensors and Actuators B: Chemical, 2017, 240: 212-219.

[33] Sharma V, Saini A K, Mobin S M. Multicolour fluorescent carbon nanoparticle probes for live cell imaging and dual palladium and mercury sensors[J]. Journal of Materials Chemistry B, 2016, 4(14): 2466-2476.

[34] R. J. T. Houk, K. J. Wallace, H. S. Hewage, etal, A colorimetric chemodosimeter for Pd(II): a method for detecting residual palladium in cross-coupling reactions. *Tetrahedron* 2008, 64, 8271 – 8278.

[35] E. Unterreitmaier, M. Schuster, Fluorometric detection of heavy metals with *N*-methyl-*N*-9-(methylanthracene)-*N*'-benzoylthiourea *Anal. Chim. Acta* 1995, 309, 339 –344.

[36] K. Kubo, Y. Miyazaki, K. Akutso, etal, A highly selective fluorescent probe for the detection of palladium(II) ion in cells and aqueous media *Heterocycles* 1999, 51, 965 –968.

[37] B. K. Pal, M. S. Rahman, A Nonextractive Quenchofluorimetric Method for the Determination of Palladium(II) at μg/L Levels Using Bathophenanthroline *Mikrochim. Acta* 1999, 131, 139 – 144.

[38] Y. J. Fang, H. Chen, Z. X. Gao, etal, Fluorescent probes for Pd^{2+} detection by poly(o-phenylenediamine) nanospheres with fluorescence enhancement Jin, *Indian J. Chem. Sect. A* 2002, 41, 521–524.

[39] A. Tamayo, L. Escriche, J. Casabo, etal, Synthesis, Complexation and Spectrofluorometric Studies of a New NS_3 Anthracene-Containing Macrocyclic Ligand *Eur. J. Inorg. Chem.* 2006, 2997 – 3004.

[40] J. R. Matthews, F. Goldoni, H. Kooijman, etal, Metal Coordination and Aggregation Properties of Chiral Polythiophenes and Polythienylethynylenes *Macromol. Rapid Commun.* 2007, 28, 1809 – 1815.

[41] L. P. Duan, Y. F. Xu, X. H. Qian, Highly sensitive and selective Pd^{2+} sensor of naphthalimide derivative based on complexation with alkynes and thio-heterocyclew *Chem. Commun*. 2008, 6339 – 6341.

[42]Li L, Gao L J, Wang J, et al. A Colorimetric and Fluorescent Sensor Based on Novel Iminocoumarin Precursor for Pd^{2+} Dectection in Aqueous Solution[J]. Journal of fluorescence, 2015, 25(5): 1165-1168.

[43] Li X, Huang H, Zhu Y, et al. Highly selective fluorescence detection of Pd 2+/4+ species based on a catalyzed aromatic Claisen rearrangement[J]. RSC Advances, 2015, 5(128): 105810-105813.

[44] Nie H, Geng J, Jing J, et al. Triphenylphosphine-assisted highly sensitive fluorescent chemosensor for ratiometric detection of palladium in solution and living cells[J]. RSC Advances, 2015, 5(118): 97121-97126.

[45] Baker M S, Phillips S T. A two-component small molecule system for activity-based detection and signal amplification: Application to the visual detection of threshold levels of Pd (II)[J]. Journal of the American Chemical Society, 2011, 133(14): 5170-5173.

[46] Liu B, Wang H, Wang T, et al. A new ratiometric ESIPT sensor for detection of palladium species in aqueous solution[J]. Chem. Commun., 2012, 48(23): 2867-2869.

[47] Zhu B, Gao C, Zhao Y, et al. A 4-hydroxynaphthalimide-derived ratiometric fluorescent chemodosimeter for imaging palladium in living cells[J]. Chemical Communications, 2011, 47(30): 8656-8658.

[48] Liang G, Cai Q, Zhu W, et al. A highly selective heterogeneous fluorescent sensor for palladium ions [J]. Analytical Methods, 2015, 7(12): 4877-4880.

[49] Haugland, R. P. Handbook of Fluorescent Probes and Research Chemicals, 6thed.Molecular Probes, Inc.: Eugene, OR 97402, and examples therein.

[50] Kim. H. N., Lee. M. H., Kim. H. J., etal, A new trend in rhodamine-based chemosensors: application of spirolactam ring-opening to sensing ions J. Chem.Soc. Rev. 2008,37, 1465–1472.

[51] Beija. M., Afonso. C. A. M., Martinho. J. M. G, Synthesis and applications of Rhodamine derivatives as fluorescent probesChem. Soc. Rev. 2009, 38,2410–2433.

[52] Chen.X. Q, Pradhan.T, Wang. F, etal, Fluorescent Chemosensors Based on Spiroring-Opening of Xanthenes and Related Derivatives *Chem. Rev*. 2012, 112, 1910–1956.

[53] Yang. Y. M., Zhao. Q., Feng. W, etal, Luminescent Chemodosimeters for Bioimaging *Chem. Rev.* **2013**, 113, 192–270 .

[54] Long Y, Zhou J, Yang M P, et al. A selective and sensitive off–on probe for palladium and its application for living cell imaging [J]. Chinese Chemical Letters, 2016, 27(2): 205-210.

[55] Valeur B, Leray I. Design principles of fluorescent molecular sensors for cation recognition [J]. Coordination Chemistry Reviews, 2000, 205(1): 3-40.

[56] Fabbrizzi L, Licchelli M, Rabaioli G, et al. The design of luminescent sensors for anions and ionisable analytes [J]. Coordination Chemistry Reviews, 2000, 205(1): 85-108..

[57] Rogers C W, Wolf M O. Luminescent molecular sensors based on analyte coordination to transition-metal complexes [J]. Coordination Chemistry Reviews, 2002, 233: 341-350.

[58] Ellis-Davies G C R. Neurobiology with caged calcium [J]. Chemical reviews, 2008, 108(5): 1603-1613..

[59]Lohar S, Banerjee A, Sahana A, et al. Selective fluorescence and naked eye detection of histidine in aqueous medium via hydrogen bonding assisted Schiff base condensation [J]. Tetrahedron Letters, 2014, 55(1): 174-176.

[60] Maszewska M, Leclaire J, Cieslak M, et al. Water-soluble polycationic dendrimers with a phosphoramidothioate backbone: preliminary studies of cytotoxicity and oligonucleotide/plasmid delivery in human cell culture [J]. Oligonucleotides, 2003, 13(4): 193-205.

[61] Tang. L. J., Li. F. F., Liu.M. H., etal, Single sensor for two metal ions: Colorimetric recognition of $Cu^{2+}$and fluorescent recognition of Hg^{2+}. *Spectrochim.Acta A* 2011, 78,1168.

[62]Caballero A, Martínez R, Lloveras V, et al. Highly selective chromogenic and redox or fluorescent sensors of Hg^{2+} in aqueous environment based on 1, 4-disubstituted azines [J]. Journal of the American Chemical Society, 2005, 127(45): 15666-15667.

[63] Wang J, Long L, Xie D, et al. Cu^{2+}-selective "Off–On" chemsensor based on the rhodamine derivative bearing 8-hydroxyquinoline moiety and its application in live cell imaging [J]. Sensors and Actuators B: Chemical, 2013, 177: 27-33.

[64] Long L, Wu Y, Wang L, et al. A fluorescent probe for hypochlorite based on the modulation of the unique rotation of the N–N single bond in acetohydrazide [J]. Chemical Communications, 2015, 51(52): 10435-10438.

[65] Nolan E M, Lippard S J. Tools and tactics for the optical detection of mercuric ion [J]. Chemical reviews, 2008, 108(9): 3443-3480.

[66] Yuan L, Lin W, Yang Y, et al. A unique class of near-infrared functional fluorescent dyes with carboxylic-acid-modulated fluorescence ON/OFF switching: rational design, synthesis, optical properties, theoretical calculations, and applications for fluorescence imaging in living animals [J]. Journal of the American Chemical Society, 2012, 134(2): 1200-1211.

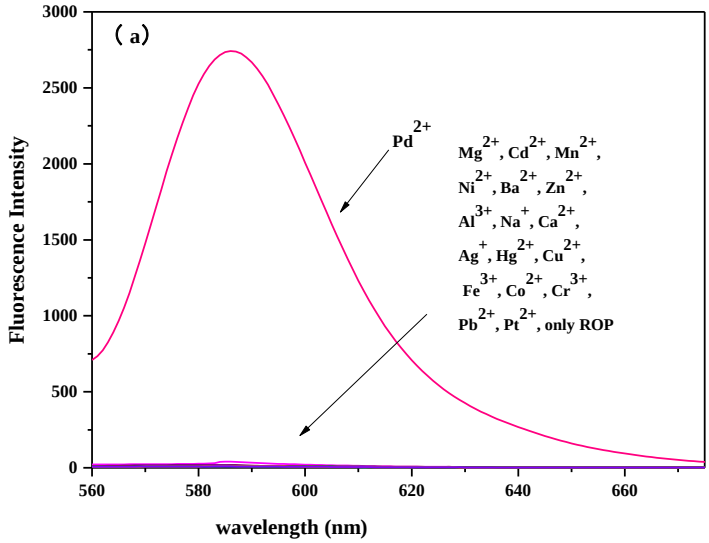
(a)
Fluorescence Intensity
wavelength (nm)
Pd2+
Mg2+, Cd2+, Mn2+,
Ni2+, Ba2+, Zn2+,
Al3+, Na+, Ca2+,
Ag+, Hg2+, Cu2+,
Fe3+, Co2+, Cr3+,
Pb2+, Pt2+, only ROP

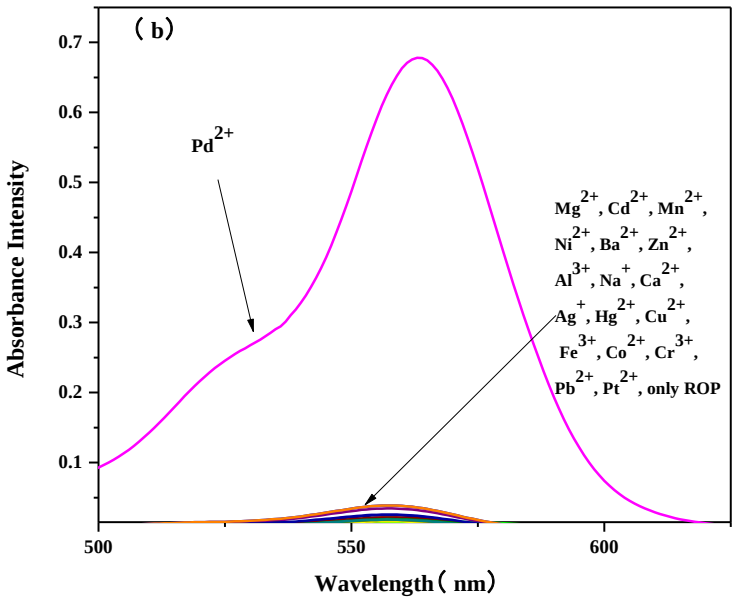
(b)
Absorbance Intensity
Wavelength(nm)
Pd2+
Mg2+, Cd2+, Mn2+,
Ni2+, Ba2+, Zn2+,
Al3+, Na+, Ca2+,
Ag+, Hg2+, Cu2+,
Fe3+, Co2+, Cr3+,
Pb2+, Pt2+, only ROP

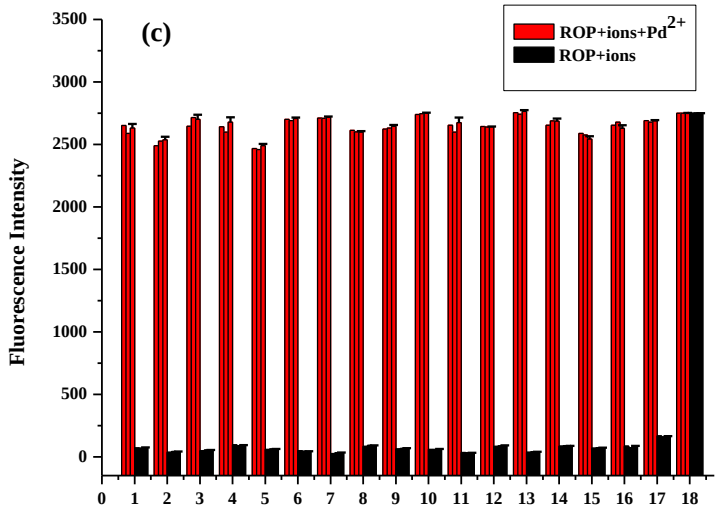

Fig.1 Fluorescence **(a)** and absorbance **(b)** spectra of **ROP** (10 μmol/L) in ethanol-water (4/6, v/v, HEPES=20mmol/L, pH=7.4) solution upon addition of various metal ions (10μmol/L), λ_{ex}=540 nm. **(c)** Fluorescence intensity changes of **ROP** (10μmol/L) upon the addition of various metal ions (10μmol/L) in the presence of Pd^{2+} (10μmol/L) in ethanol-water (4/6, v/v, HEPES=20mmol/L, pH=7.4) solution. The black bars represent the fluorescence response of **ROP** and competing ions: 1.Al^{3+}, 2.Na^{+}, 3.Ca^{2+}, 4.Mg^{2+}, 5.Cd^{2+}, 6.Mn^{2+}, 7.Ni^{2+}, 8.Ba^{2+}, 9.Zn^{2+}, 10.Co^{2+}, 11.Cr^{3+}, 12.Pb^{2+}, 13.Ag^{+}, 14.Fe^{3+}, 15.Hg^{2+}, 16.Cu^{2+}, 17.Pt^{2+}, 18.Pd^{2+}. The red bars represent the subsequent addition of 10μmol/L Pd^{2+} to the above solutions. Error bar=RSD (n=3)

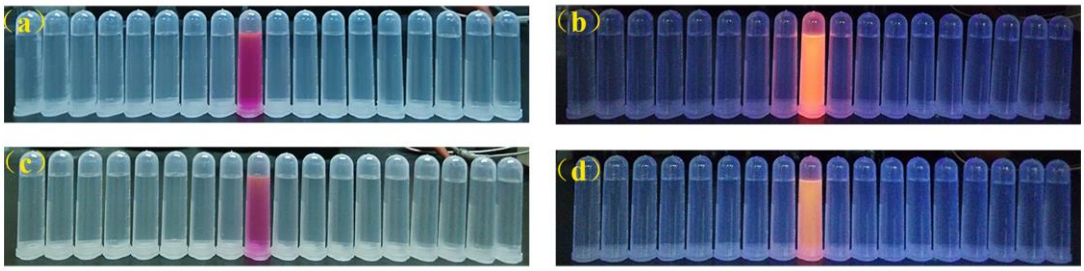

Fig.2 (a) and (c) the color change of the probes **ROP** and **ROM** in different metal ions(1. Na^{+}, 2. Al^{3+}, 3.Ca^{2+}, 4.Mg^{2+}, 5.Cd^{2+}, 6.Mn^{2+}, 7.Ni^{2+}, 8.Ba^{2+}, 9. Pd^{2+}, 10. Cr^{3+} 11.Co^{2+}, 12. Pt^{2+}, 13.Pb^{2+}, 14.Ag^{+}, 15.Fe^{3+}, 16.Hg^{2+}, 17.Cu^{2+}, 18. Zn^{2+}); (b) and (d) the fluorescence change of the probes **ROP** and **ROM** in different metal ions(both 10μmmol/L)

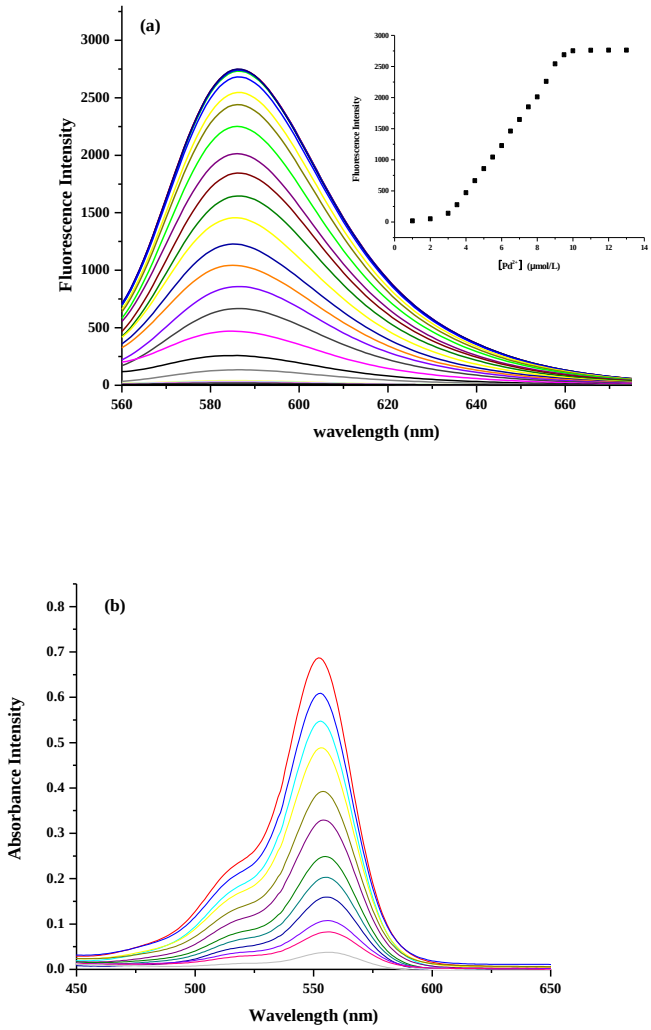

Fig.3 (a) Fluorescence intensity changes of **ROP** (10μmol/L) upon addition of Pd^{2+} in ethanol-water (4/6, v/v, HEPES=20mmol/L, pH=7.4) solution. Inset: Changes in the emission intensity at 583nm. **(b)** Absorbance intensity changers of **ROP** (10μmol/L) upon addition of Pd^{2+} in ethanol-water (4/6, v/v, HEPES=20mmol/L, pH=7.4) solution.

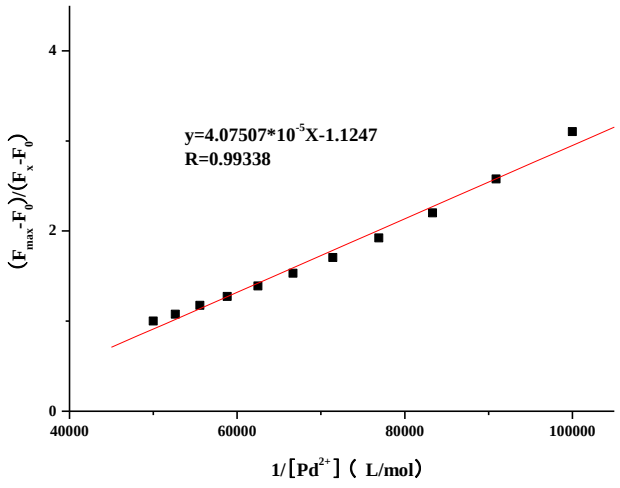

Fig.4 Determination of binding constant of **ROP** (10 μmol/L) with Pd^{2+} (10 μmol/L) using Benesi–Hildebrand equation.

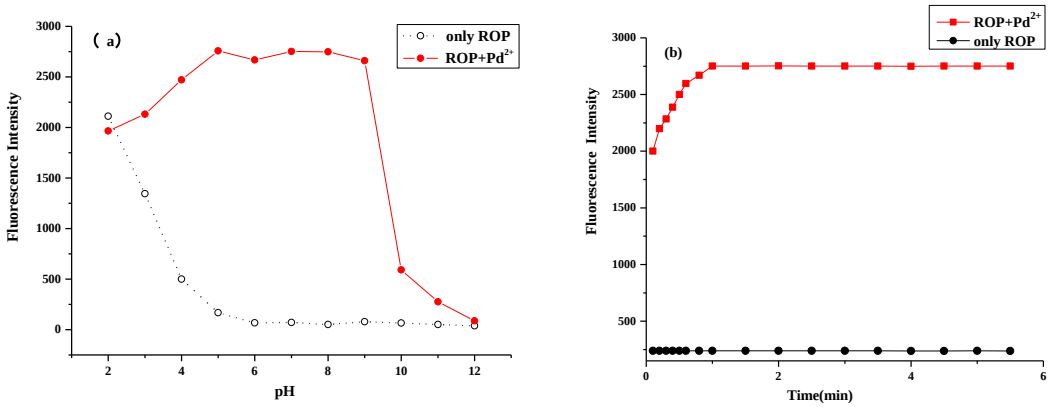

Fig 5 (a) Effect of pH on **ROP** (10 μmol/L) recognition Pd^{2+} (the pH of solution was adjusted by aqueous solution of NaOH (1mol/L) and HCl (1mol/L). (b) Effect of time on probe **ROP** (10 μmol/L) recognition Pd^{2+} (λ_{ex}=540 nm, λ_{em}=583nm)

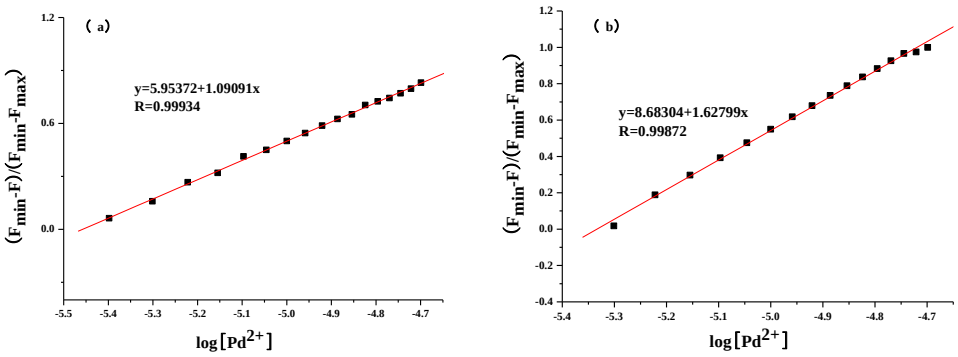

Fig.6. The plots of $(F_{min} - F) / (F_{min} - F_{max})$ versus $\log [Pd^{2+}]$ for the probes **ROP (a)** and **ROM (b)**.

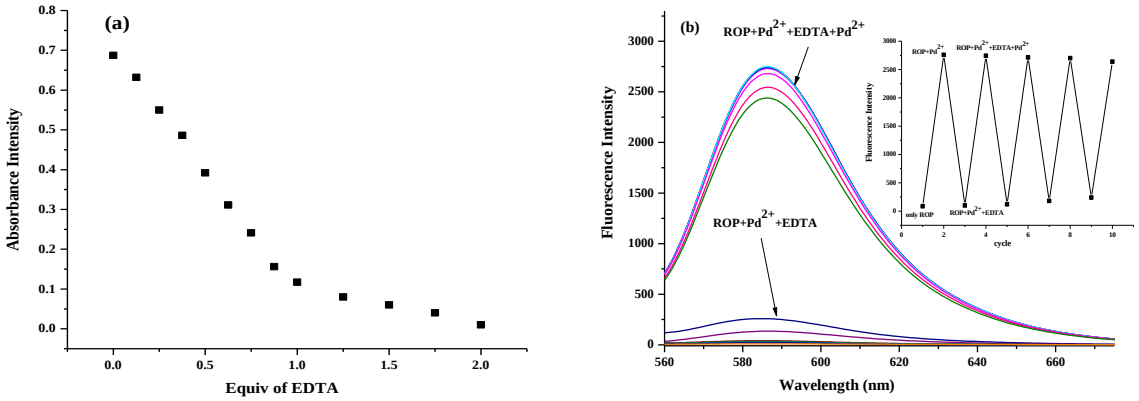

Fig.7 (a) Absorbance intensity changes at 550 nm of **ROP** (10 μmol/L) upon the addition of each equiv of EDTA with the presence of Pd^{2+} in ethanol-water (4/6, v/v, HEPES=20mmol/L, pH=7.4) solution. (b) Fluorescence intensity of probe **ROP**+Pd^{2+}as a function of EDTA concentration in ethanol-water (4/6, v/v, HEPES=20mmol/L, pH=7.4) solution. Inset: fluorescence intensity at 583nm for four cycles of the switching process.

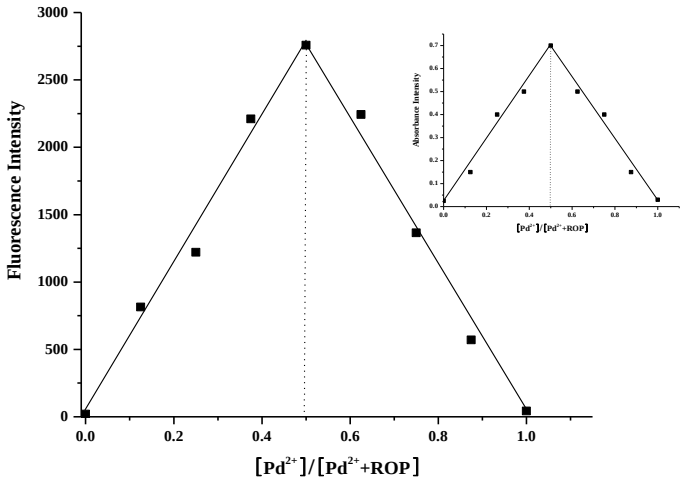

Fig.8 Job's plot of **ROP** and Pd^{2+} (The total concentration was 10 μmol/L).

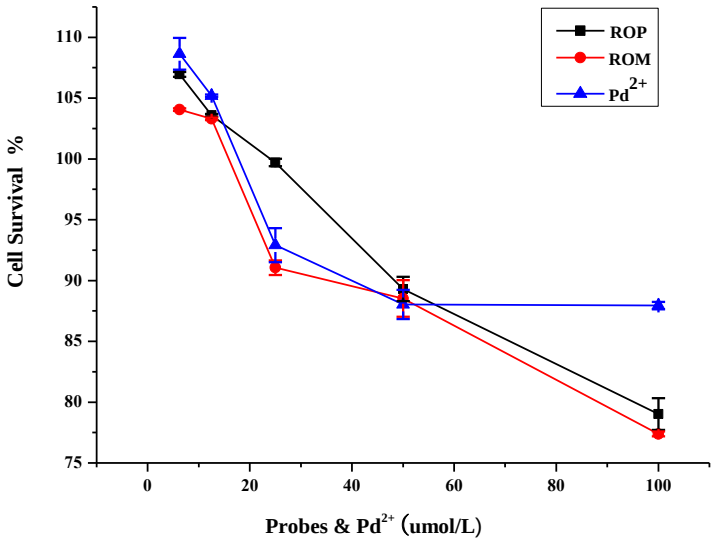

Fig. 9 HepG2 living cells viability of ROP, ROM and Pd^{2+} were quantified by the MTT assay (mean ± SD).

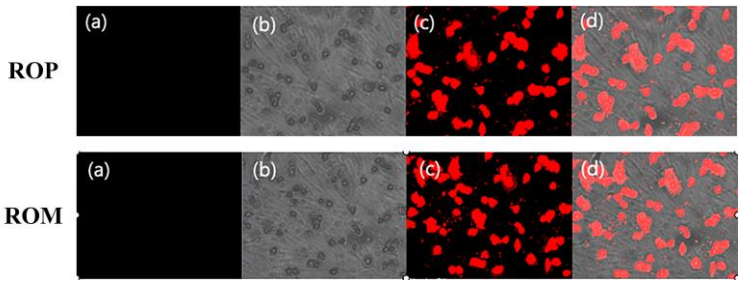

Fig.10 Probe **ROP** and **ROM** for Pd^{2+} fluorescence images in HepG2 living cells. Fluorescence images of HepG2 cells treated with probes (10 μmol/L) in either the absence (**a**) or the presence (**c**) of 10 μmol/L Pd^{2+} for 1h at 37 °C. (**b**) Bright-field image of cells shown in panel. (**d**) Overlay image of (**b**) and (**c**).

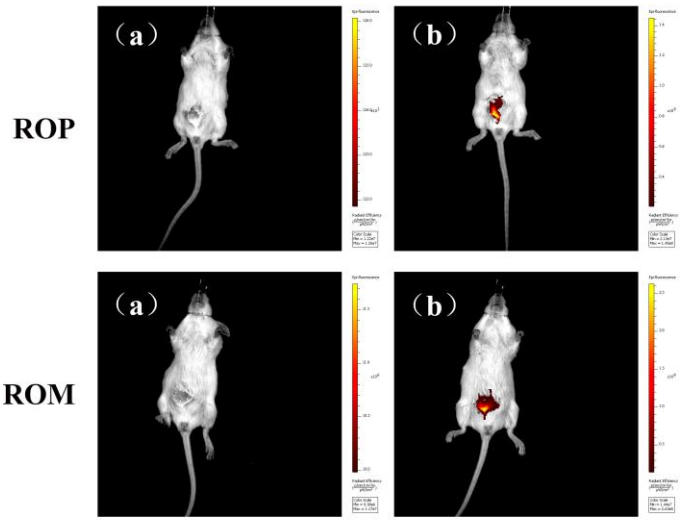

Fig. 11 Representative fluorescence images for the mouse. ((a).only injection with 10 μmol/L, 5 μL ROP and ROM and (b) .after injection with 10 μmol/L, 5 μL Pd^{2+}.)The mice were imaged using IVIS DPECTRUM, with an excitation filter 550 nm and an emission range = 580-600 nm.

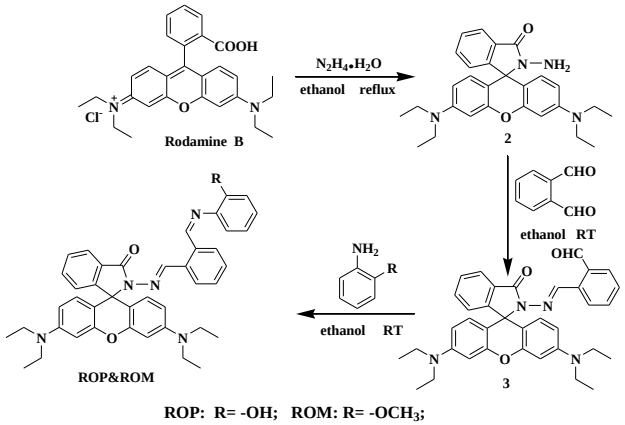

Scheme 1 Synthesis of ROP and ROM

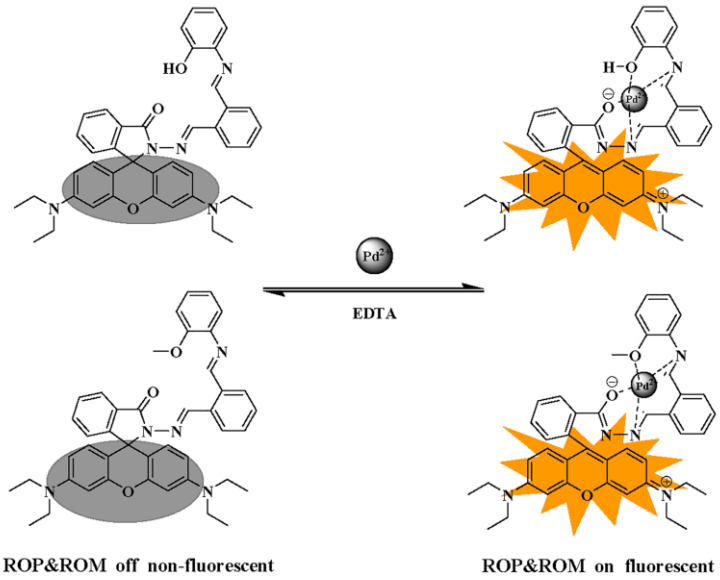

Scheme 2 The most likely binding modes between the probes **ROP&ROM** and Pd^{2+}